FERMILAB-PROPOSAL-0829 10/18/93

P829: Continued Study of Heavy Flavors at TPL

B. Meadows, M. Sokoloff[*]
University of Cincinatti

J.A. Appel, D. Christian[*], M. Halling, S. Kwan
Fermi National Accelerator Laboratory

R. Burnstein, H. Rubin
Illinois Institute of Technology

M.C. Berisso, E.P. Hartouni, M.N. Kreisler
University of Massachusetts

G. Herrera
Cinvestav, Mexico

M.V. Purohit
Princeton University

A. d'Oliveira[1], A. Fernandez
Universidad Autonoma de Puebla, Mexico
[1] *On leave from UNESP/Sao Paulo/Brazil*

D. Ashery, J. Lichtenstadt
Tel Aviv University

A. Napier
Tufts University

M. Sheaff
University of Wisconsin

R. Harr, P. Karchin, C. Kennedy
Yale University

S. Bracker
317 *Belsize Dr., Toronto, Ont.*

[*] Co-spokesmen

829

Continued Study of Heavy Flavors at TPL

Contents

1. Introduction
2. The Detector
3. Status of E791
4. P829 Goals
5. Reaching the Goals
6. Comparison With Other Experiments
7. Resources Required
8. Summary

1. Introduction

The Tagged Photon Laboratory (TPL) has been home to four experiments studying charm in the past 15 years. A short summary of these experiments' characteristics and their charm signals is given in Table 1-1. While the goals of these experiments and the particular decay modes studied have varied, and the signal-to-background ratios for the experiments have not been uniform, one may reasonably conclude that the final charm samples have grown dramatically with time largely because the number of events recorded on tape has increased. We now propose to integrate the best elements of the high-rate E690 spectrometer and the existing E791 spectrometer to extend this program of studying heavy quark physics. We plan to increase the charm yield, compared to E791, by a factor between 15 and 25. The cost will be modest because most of the needed equipment exists, and the likelihood that the new experiment will succeed is high because the key elements of the "new" spectrometer have been used successfully in previous experiments. We will increase the final charm sample relative to E791 by increasing the rate at which we write data to tape, by recording data for a longer period of time, by running at a higher instantaneous luminosity and triggering more tightly on transverse energy (E_T) to accept a sample of events more enriched in charm, and by improving the hardware so that our reconstruction efficiency increases.

The proposed experiment will accumulate the world's largest sample of reconstructed charm to study various topics in heavy quark physics. Foremost among these will be the detailed properties of charmed meson decays. We will measure the form factors and polarization structure of D^0, D^+, and D_s semi-leptonic decays to vector mesons with sufficient precision to constrain theoretical models stringently. Looking at Cabibbo-allowed and Cabibbo-suppressed semi-leptonic decays, we will determine the ratio $|V_{cd}|/|V_{cs}|$ with 1% - 2% statistical error. We will determine the rates of hadronic double Cabibbo-suppressed decays (DCSD's) with the same precision as did E691 and MARK III for Cabibbo-allowed decays, and as E791 will do for single Cabibbo-suppressed decays. We will search for D^0 - $\overline{D}^0$ mixing at

the level of a few times 10^{-4}. We will search for direct CP violation in several D^0 and D^+ decay modes with a sensitivity of a few percent. We will search for flavor-changing-neutral-currents (FCNC's) in decay modes such as $D^+ \to \pi^+\mu^-\mu^+$ with a sensitivity of order 10^{-5}. We will study the spectroscopy of excited charmed meson states with high statistics, and we will study the production of charm by hadrons. Similarly, we will study the decay properties of charmed baryons and their excited states, and also their production. In addition, we expect to observe several B signals which will allow us to to study topics in both production and decay physics.

To operate at higher rates with higher efficiency, we will replace the E791 drift chambers with the E690 drift chambers and their readout electronics. We will use the existing E791 SMD planes, but will replace the oldest SMD electronics to operate more cleanly with less dead time. We will use the basic data acquisition system that served E791 so well, but we will expand its capacity and speed to handle approximately twice the total bandwidth with substantially less dead time per event. We will continue to use the two threshold Čerenkov counters in TPL which separate pions from kaons between 6 GeV/c and 40 GeV/c, and we will add the E690 Čerenkov counter which has a 2.6 GeV/c threshold for pions. Modest improvements to the muon detector will increase acceptance at higher angles and will reduce backgrounds due to punch-through substantially. Altogether, by running at a higher instantaneous luminosity with a modified target configuration for 3×10^6 seconds, we expect to reconstruct a charm sample with 15 to 25 times the statistics of E791.

Table 1-1

Experiment	Year Data Taken	Beam & Energy	Hadronic Events	Charm Signal Reconstructed	Charm Rate
E516	1980	$< E_\gamma >= 105$ GeV	7 million	150	21
E691	1985	$< E_\gamma >= 145$ GeV	100 million	10000	100
E769	1987	$E_{\pi,K,p} = 250$ GeV	400 million	4000	10
E791	1991	$E_\pi = 500$ GeV	20 billion	200000	10

A short history of TPL: E516 and E691 were photoproduction experiments. E516 published several papers reporting charm signals, mostly on production topics. E691 added a silicon vertex detector and observed much cleaner signals. It published several papers on photoproduction of charm and many on charm decay and spectroscopy topics. E769 was designed to study hadroproduction of charm using a variety of beams. It has published several papers on this physics. E791 is now analyzing its data, and its physics projections are described in the body of this proposal. The last column gives the rate of reconstructed charm per million hadronic interactions recorded on tape. The triggering varied from one experiment to another, so this is a limited figure of merit.

2. The Detector

Figures 2-1 and 2-2 show the spectrometer used in TPL for E791. Figure 2-3 shows how we propose to use components of the E690 spectrometer to replace almost all of the drift chambers used in E791. It also shows where we will position the E690 Čerenkov counter. We plan to run with essentially the same pion beam as was used by E791. This means that we can use E791 data and the E791 Monte Carlo to reliably quantify the strengths and weaknesses of our new spectrometer.

The proposed configuration maintains the same acceptance through the first spectrometer magnet as the E791 spectrometer had. The aperture of the wire chamber immediately downstream of the second magnet is slightly smaller than in E791. The most downstream chamber is approximately one-half as large as the chamber used in E791. We have examined the consequences of these reduced apertures by plotting the momentum spectrum of tracks from $D \rightarrow K2\pi$ decays measured by E791 which fall inside and outside of the new chamber apertures. As shown in Figures 2-4 through 2-6, only 2% of these charm decay tracks fall outside of the new chamber aperture just downstream of the second magnet. Moreover, essentially none of these 2% has momentum greater than 15 GeV/c. 26% of the charm decay tracks fall outside the aperture of the most downstream chamber, but essentially none of these 26% has momentum greater than 30 GeV/c. Tracks with momentum less than 15 GeV/c will be measured well by the chambers on either side of the first magnet, and tracks with momentum in the range 15-30 GeV/c will be measured well using both magnets without the full lever arm provided by the most downstream chamber.

In the balance of this section, we will describe each detector element, and review which elements have been used in the past in TPL, which exist as part of E690, and which will be new. We will point out the features of the new detector which will allow us to take better quality data faster than has been possible in the past.

2.1. Vertex Detector

We propose to maintain the configuration of SMD planes used by E791 in the new spectrometer with only one modification. The system consists of 17 silicon microstrip planes located downstream of a thin scintillation counter used to select interactions in the target. The vertex detector covers a square aperture with 125 mrad half angle. 11 of the 17 planes are 5cm square detectors. The first two planes (1 x & 1 y view) contain a central region of 25 micron pitch strips and outer regions of 50 micron pitch strips. The next 9 planes have 50 micron pitch strips and are arranged as triplets (3 views). The last 6 planes are larger detectors, which cover close to 10cm $\times$ 10cm, and are arranged as two triplets. These also have 50 micron pitch strips. Every strip is read out in a central region. Outside of the central region, every fourth strip is read out, yielding an effective pitch of 200 microns. The strips which are not read out are also not grounded and share charge by capacitive coupling to the nearest instrumented strip (ref: Kodama et al., NIM A289, 1990, 146-167).

We propose to add two more high resolution (25/50 micron pitch) SMD planes just upstream of the existing vertex detector. These planes will provide additional redundancy for pattern recognition as well as additional measurement resolution.

2.2. Tracking/Magnetic Spectrometer

Almost all of the wire chambers which will be used come from E690. The exceptions are the two drift chamber assemblies designated D2' and D3' (3 planes each), which were built for E691. The E690 chambers have proven their ability to provide good measurement resolution (less than 200 micron rms error), with high efficiency (greater than 99% per plane), at interaction rates higher than proposed for this experiment. The E690 chambers are much more highly segmented than the chambers which have been used in TPL in the past (see Table 2-1). Fine segmentation and high per plane efficiency will yield higher track reconstruction efficiency than achieved by E791, especially for tracks near the beam. This will translate directly

into better charm reconstruction efficiency. We have not yet simulated the effect of better segmentation, but a Monte Carlo simulation in which it was assumed that the existing TPL chambers were efficient near the beam resulted in a 26% increase in the number of $D \rightarrow K2\pi$ decays reconstructed. At large x_F the gain was more dramatic: the number of decays reconstructed in the range $.3 < x_F < .4$ increased by a factor of 1.9, and the number in the range $.4 < x_F < .5$ increased by a factor of 2.5. This will be particularly significant for charm production studies.

2.3. Čerenkov Counters

The E791 spectrometer included two multicell threshold Čerenkov counters, with pion thresholds of 5.6 GeV/c and 10.5 GeV/c. Both of these counters covered approximately 65 mrad vertically, and 130 mrad horizontally (D. Bartlett, et. al, NIM A260, p55, 1987). We propose to add a third Čerenkov counter, with a pion threshold of 2.57 GeV/c, between the two analysis magnets. This Čerenkov counter was used in E690, and provided 10-30 photoelectrons for a $\beta = 1$ particle. The counter was designed to be used as an upstream element in a multiparticle spectrometer. Its mirrors are made of 1 mm thick glass and are supported on a lightweight paper honeycomb panel with carbon fiber reinforced skins. The volume downstream of the mirrors closest to the beam can be filled with Helium gas. The entire counter assembly, including entrance and exit windows, Freon 114 radiator, mirrors & mirror mounts, and helium bag, represents 2.9% of a radiation length of material, approximately half of which is in the Freon 114.

The new Čerenkov counter will extend the range of particle identification to lower momentum, and will provide this information for the full acceptance of the first analysis magnet, rather than just the acceptance of the second analysis magnet. It should be noted that in addition to π, K, p identification, this Čerenkov counter will provide electron identification for electrons with momenta in a range from approximately 1 GeV/c to 2.6 GeV/c. This will be valuable in the study of semi-leptonic D decays. It may also give us the opportunity to measure radiative D and D_s decays (using a single converted photon) with mass resolution superior

to CLEO II. We note, for example, that E706/E672 has successfully resolved χ_1 from χ_2 using converted photons, even though they cannot resolve these two states using photons measured in the liquid argon colorimeter. Finally, in the very high statistics sample we will collect, it should be possible to tag and study $D^* \rightarrow D\pi^0$ transitions using events in which both photons from the π^0 convert. It *may* be possible to tag $D^* \rightarrow D\pi^0$ transitions in events in which only one photon converts by requiring that photon to be nearly co-linear with the reconstructed D meson. The comparative merits of these approaches will be studied using a Monte Carlo simulation of the proposed spectrometer.

2.4. Calorimetry

We propose to continue using the electromagnetic and hadron calorimeters used in all of the previous TPL heavy flavor experiments. The electromagnetic calorimeter (labelled SLIC in Figure 2-1) is a 60 layer lead-liquid scintillator shower detector which contains a total of 20 radiation lengths of material (ref: V.K. Bharadwaj et al., NIM 228 (1985) 283-289). It is read out in strips using wavelength shifter bars in three views using a total of 334 photomultiplier tubes. The SLIC provides good electron identification, and the software now allows for electrons with momentum above 3 GeV/c. Note that this threshold is defined by geometrical acceptance, and is much lower than used in analysis before E791.

The hadron calorimeter (Hadrometer) is a 36 layer steel-acrylic scintillator shower detector which contains a total of 6 absorption lengths of material (ref: J.A. Appel et al., NIM A243 (1986) 361-373). The scintillators are constructed using 14.3 cm wide strips. Horizontal and vertical strips alternate throughout the thickness of the detector. The light is collected by conventional light pipes. Light from 9 layers is delivered to a single phototube, so that the read out is segmented into x and y strips and two sections in the beam direction. The SLIC contains 1.5 absorption lengths of material, so hadronic energy is measured with a weighted sum of SLIC and Hadrometer measurements.

The most important function of the Hadrometer is its contribution to the E_T trigger. The E_T trigger is formed using weighted analog sums of dynode signals from the phototubes of the SLIC and the Hadrometer. The quantities used to calculate E_T on-line were digitized and written to tape during E791 (and previous runs). This has allowed us to quantify what fraction of the data collected by E791 would have been rejected by higher E_T trigger requirements, as well as what fraction of the events containing reconstructed charmed particles would survive.

2.5. Muon System

The muon identification system used in the past in TPL has been a very simple system consisting of coarsely segmented scintillation hodoscopes placed behind an iron shield wall located downstream of the Hadrometer. This system can be significantly upgraded at very low cost. At the very least we will add more shielding in the presently empty space between the calorimetry and the muon wall. This will reduce the rate of punch-throughs, which presently make muon identification problematic above 70 GeV/c. Depending on the availability of manpower, we would also like to replace the oldest scintillation counter hodoscope with a hodoscope with slightly greater segmentation and extend the other scintillation counter hodoscope so that it covers the full vertical aperture of the second analysis magnet. We would also like to add one station of coarse tracking detectors between the existing muon shielding walls, and one station behind the existing muon hodoscopes. Even coarse tracking will allow us to extend the range of muon identification from the current lower limit of approximately 10 GeV/c to closer to 5 GeV/c. The current limit is due to the high probability of accidental association of a low energy muon with hits in the muon hodoscopes due to the large multiple scattering radius of the low energy tracks. These extensions of the current muon identification capabilities would extend the reach of the new experiment for the measurement of semi-muonic decays, and for rare decays such as $D^+ \rightarrow \pi^+\mu^+\mu^-$ (a flavor changing neutral current decay).

2.6. Beam Measurement

E791 measured the incoming pion beam using 8 PWC planes and 6 25-micron pitch SMD planes. This system worked well. We expect it to continue to work well in the proposed experiment without modification.

2.7. Front End Electronics

Vertex Detector Electronics

The E791 silicon microstrip detector used three different types of front end electronics. In each case strip signals were amplified, discriminated, and latched. All of the latches were read out through shift registers; the latch contents were loaded in parallel into a shift register, and then read out in series into a scanner which generated a hit address for every hit channel by incrementing an address counter with the same clock used to shift the latch bits out of the shift register. The read out deadtime of this system was dominated by the time required to shift the latch contents out of the shift registers: 256 bits/12 MHz = 21.3 microseconds.

E791 actually operated with a 50 microsecond deadtime, because one of the three systems of SMD front end electronics (the "E691" system) was prone to oscillations. These oscillations took 20-25 microseconds after the scanner read out was completed to damp out.

We propose to reduce the SMD read out deadtime to less than 13 microseconds. This will be done by splitting the 256 bit shift registers into twice as many 128 bit shift registers, and doubling the number of parallel paths used in the process of encoding latch bit patterns into a list of hit strips. These changes will be accomplished by using a larger number of Princeton Scanner modules. We must also solve the oscillation problem in the E691 SMD front end system. This we propose to do by replacing the MSD2 preamplifier cards with a preamplifier based on the Fermilab QPA02 developed for E771 and E789 (T.Zimmerman, IEEE Trans. Nucl. Sci. 37, 439-443), and by replacing the E691 discriminator/latch cards with a design very similar to that used to latch the E791 beam SMD signals.

Wire Chamber Electronics

The proposed spectrometer will include a total of 13,472 instrumented drift chamber wires. The two chambers used in E791 (1184 channels; 21 TDC's) will be read out using the system of FASTBUS TDC's which was installed for E791. In order to guarantee a read out deadtime of less than 12 microseconds, these TDC's will be spread over four FASTBUS crates. The balance of the E791 FASTBUS TDC system (more than 5000 TDC channels and 6 FASTBUS crates, controllers, etc.) will not be required by the new experiment. All of the chambers previously used in E690 (12,288 channels) will be read out using E690 drift chamber electronics.

The E690 drift chamber read out system is entirely "homemade;" it was all designed at Nevis Labs, and was built mostly at the University of Massachusetts. The system consists of preamplifiers, mounted on the wire chambers, which drive differential signals over short cables to leading edge discriminators located next to the detector. The discriminators drive differential ECL signals over long delay cables to TDC's. The TDC's are simple digital modules; the arrival of a discriminator pulse latches the state of a Gray code counter with a 2.54 nsec. least count. There is no conversion deadtime. Up to 16 32-channel TDC's can fit in a single crate. The system requires a gate, but no other external read out control. The trailing edge of the gate triggers the data-driven read out of all hit channels. All crates are read out simultaneously at a rate of 50 nsec per hit into buffer memories located in "segmenters" in each crate. The system is dead only during read out into the segmenters. Segmenter outputs can be daisy-chained to provide whatever number of parallel read out paths is desired. If five parallel read out paths are used to load TDC information into the VDAS FIFO's (as was the case for E791), the read out deadtime of this system will be approximately 5 microseconds.

Phototube Electronics (FERA ADC's)

A total of 39 16-channel LeCroy FERA ADC's were used in E791. These modules digitized signals from the Čerenkov counters, the liquid scintillator electromagnetic calorimeter, the hadron calorimeter, and various quantities used for

trigger logic (E_T partial sums, etc.). These modules were housed in two CAMAC Crates. The typical read out deadtime was 25-30 microseconds. Approximately 8.2 μsecs of this total was taken by 10 bit A/D conversion and on-module pedestal subtraction. A typical event consisted of 320 16-bit words of information (module header words and pulse heights), about half of which was generated in each of the two crates. Information from the two crates was read out in parallel through two "Damn Yankee" controllers into the VDAS FIFO system. The read out deadtime was dominated by the time required to move data from the FERA ADC's into the Damn Yankee controllers (the Damn Yankee modules contain a pipeline buffer). Data could be clocked from FERA ADC's into the Damn Yankees with a 110 nsec clock; the typical event took 160*110 nsec = 17.6 μsec to transfer.

We propose to reduce the read out deadtime of the FERA ADC system by increasing the number of parallel read out paths from 2 to 8. This will reduce the time required to transfer data from the ADC's to the Damn Yankees to approximately 40*110 nsec = 4.4 μsec. The overall ADC deadtime will be reduced to 8.2+4.4 = 12.6 μsec.

2.8. VME Event Building/Tape Writing System

E791 wrote an unprecedented number of events to high density 8mm video tape using a highly parallel system implemented in VME (S. Amato, et al, NIM A324 (1993), 535-542). We propose to double the tape writing speed capacity of the E791 taping system by replacing the 42 Exabyte 8200 tape drives (1/4 MB/sec) with 42 Exabyte 8500 tape drives (1/2 MB/sec). We will preserve the VME crate structure of the E791 taping system, but we will replace the 54 ACP-I modules which were used to control the tape writing system, and as event builders, with a smaller number of much faster commercial VME computers. We will build 24 more EBI modules to accept data from the 4 new VDAS subsystems. We will either write data to tape through SCSI controllers on the commercial VME computers, or through VME/SCSI tape controllers, as was done in E791.

2.9. VDAS FIFO System

As in previous experiments in TPL, we will collect data faster during the 23 second Tevatron spill than it can be written to tape. Enough data will be buffered during the spill to keep the tape drives streaming between spills as well as during the spill. As in E791, data will be stored in very large buffers designed and built at Fermilab called VDAS FIFO's. The VDAS FIFO system used in E791 consisted of 8 subsystems, each with a capacity of 80 MBytes, for a total of 640 MBytes. This was more than enough buffer memory to allow E791 to perform a small amount of data sparsification in ACP-I computers located after the VDAS FIFO's in the read out pipeline, and still keep the 42 Exabyte 8200 tape drives streaming for the entire 34 second time period between spills.

We propose to build 4 more VDAS subsystems. This will increase the FIFO capacity to 960 Mbytes. This amount of buffer memory should allow the experiment to write data continuously to 42 Exabyte 8500 tape drives at an aggregate rate of 21 MBytes/second.

Table 2-1

Chambers used in E791		Replacement Chambers	
Chamber	Wire Spacing	Chamber	Wire Spacing
D1	4.5mm (8 planes)	CH1	1.5mm (4 planes)
PWC	2.0mm (2 planes)	CH2	2.0mm (4 planes)
		CH3	2.0mm (4 planes)
D2,D2′	9.0mm (12 planes)	CH4	3.0mm (4 planes)
		CH5	3.5mm (4 planes)
D3,D2′	15.0mm (12 planes)	CH6	3.0mm (4 planes)
		D2′	9.0mm (3 planes)
		D3′	15.0mm (3 planes)
D4	30.0mm (3 planes)	CH7	3.0mm (4 planes)

Figure 2-1

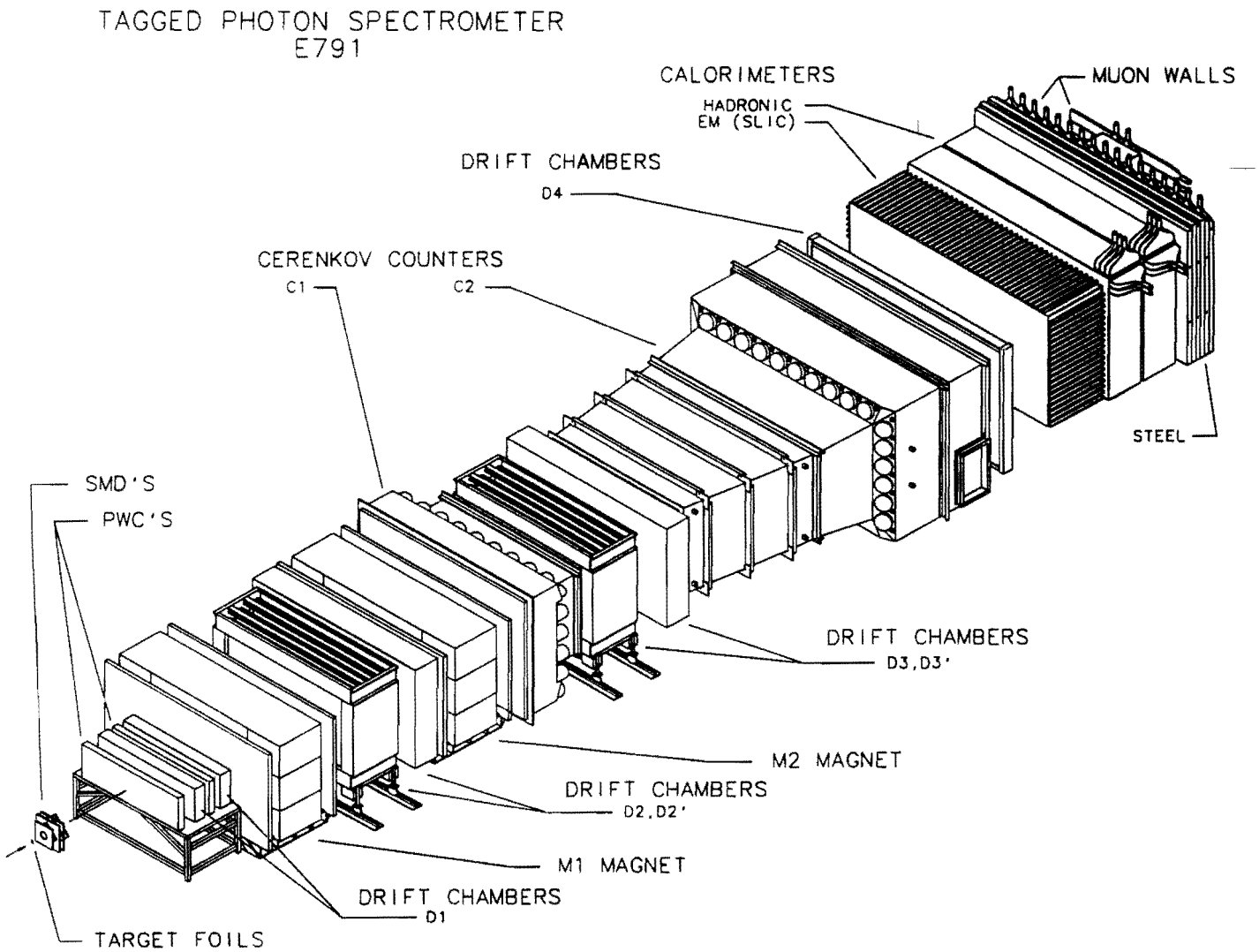
TAGGED PHOTON SPECTROMETER
E791
CALORIMETERS
HADRONIC
EM (SLIC)
MUON WALLS
DRIFT CHAMBERS
D4
CERENKOV COUNTERS
C1
C2
STEEL
SMD'S
PWC'S
DRIFT CHAMBERS
D3,D3'
M2 MAGNET
DRIFT CHAMBERS
D2,D2'
M1 MAGNET
DRIFT CHAMBERS
D1
TARGET FOILS

Figure 2-2

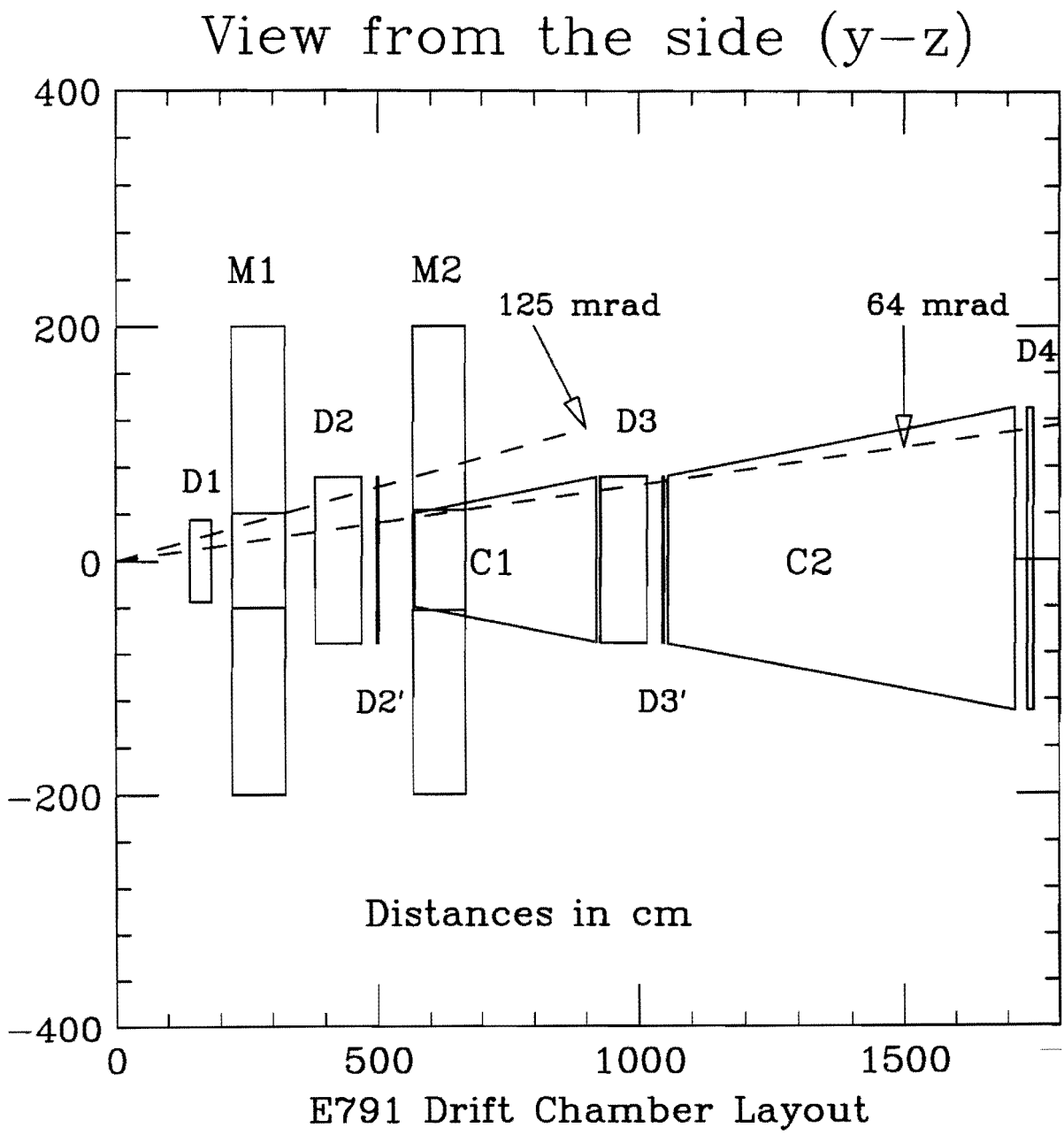
View from the side (y−z)
400
200
0
−200
−400
0
500
1000
1500
M1
M2
125 mrad
64 mrad
D4
D2
D3
D1
C1
C2
D2'
D3'
Distances in cm
E791 Drift Chamber Layout

Figure 2-3

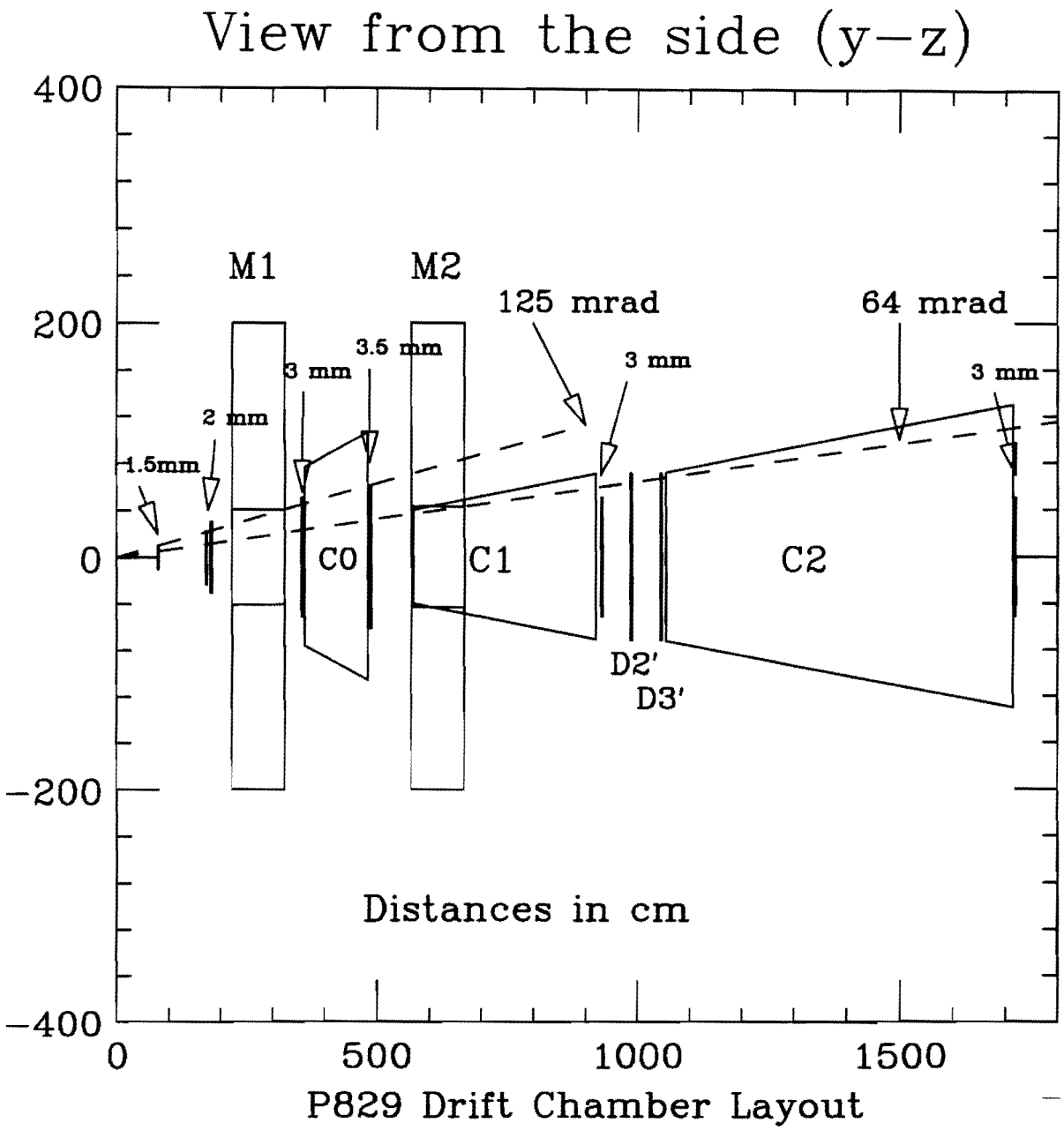
View from the side (y−z)
400
200
0
−200
−400
0
500
1000
1500
M1
M2
125 mrad
64 mrad
3.5 mm
3 mm
3 mm
3 mm
2 mm
1.5mm
C0
C1
C2
D2'
D3'
Distances in cm
P829 Drift Chamber Layout

Figure 2-4

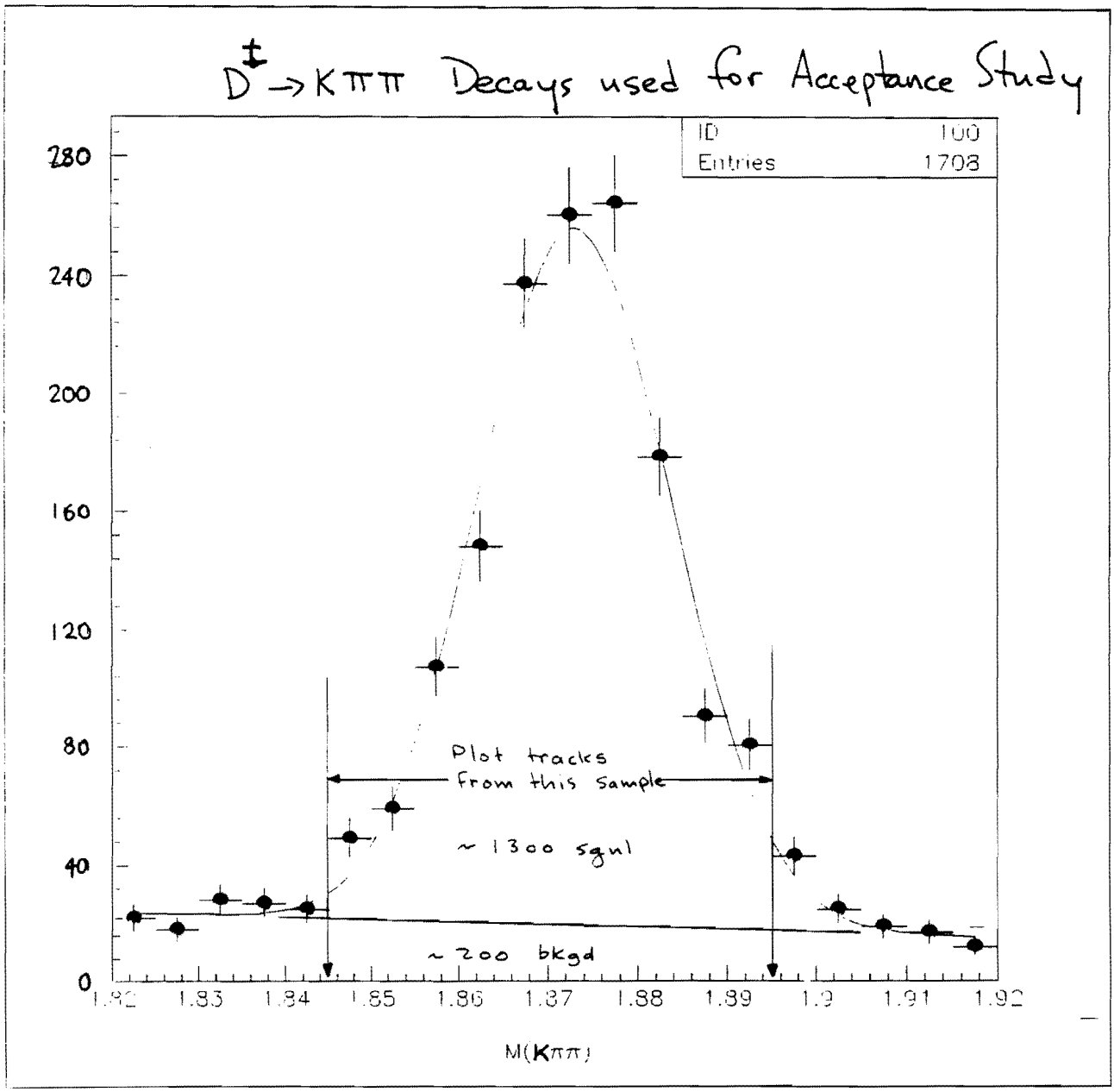

N.B. P > 9 GeV/c for all tracks

Figure 2-5

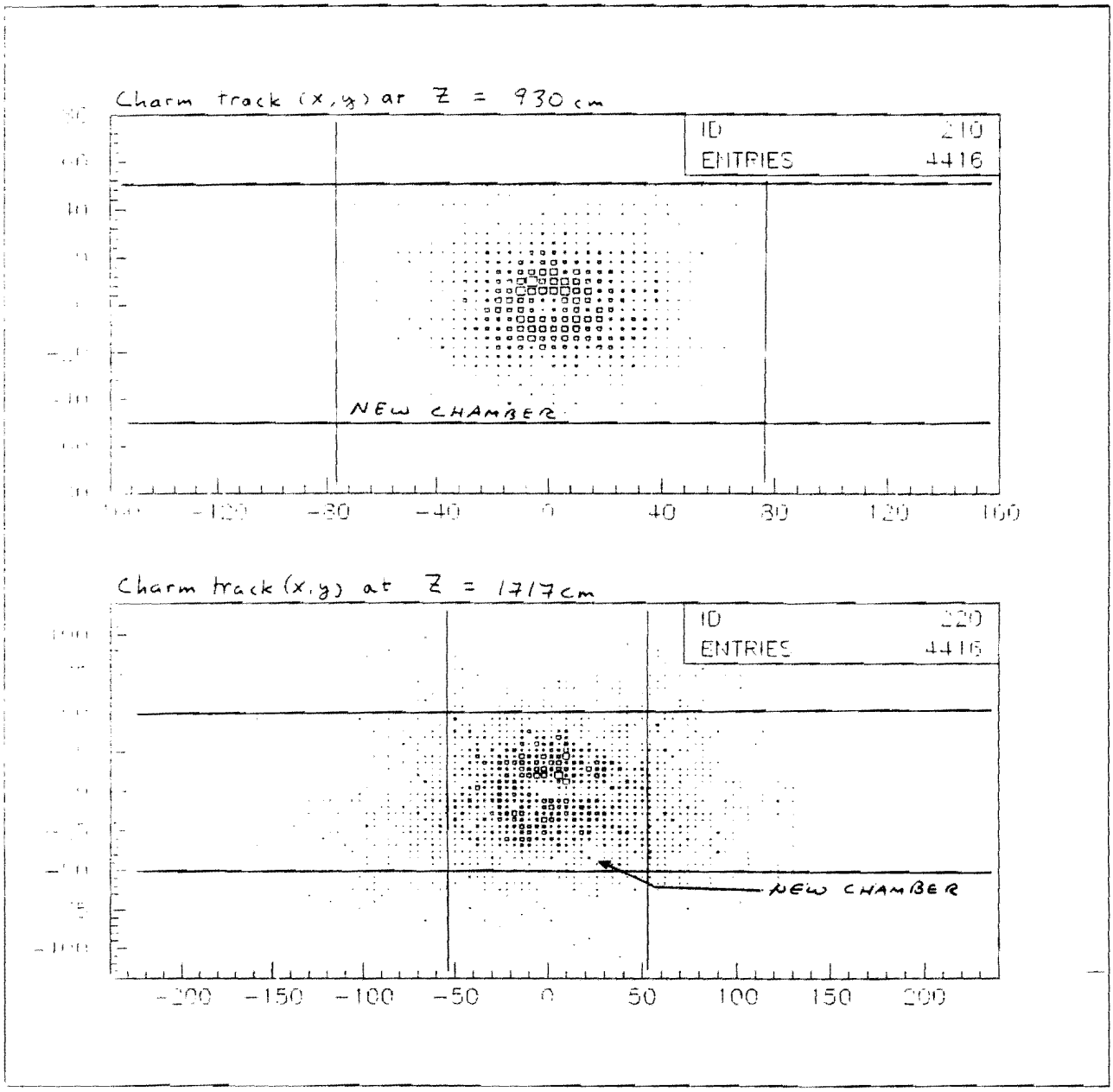
Charm track (x,y) at Z = 930 cm
ID 210
ENTRIES 4416
NEW CHAMBER
-120 -80 -40 0 40 80 120 160
Charm track (x,y) at Z = 1717 cm
ID 220
ENTRIES 4416
NEW CHAMBER
-200 -150 -100 -50 0 50 100 150 200

Figure 2-6

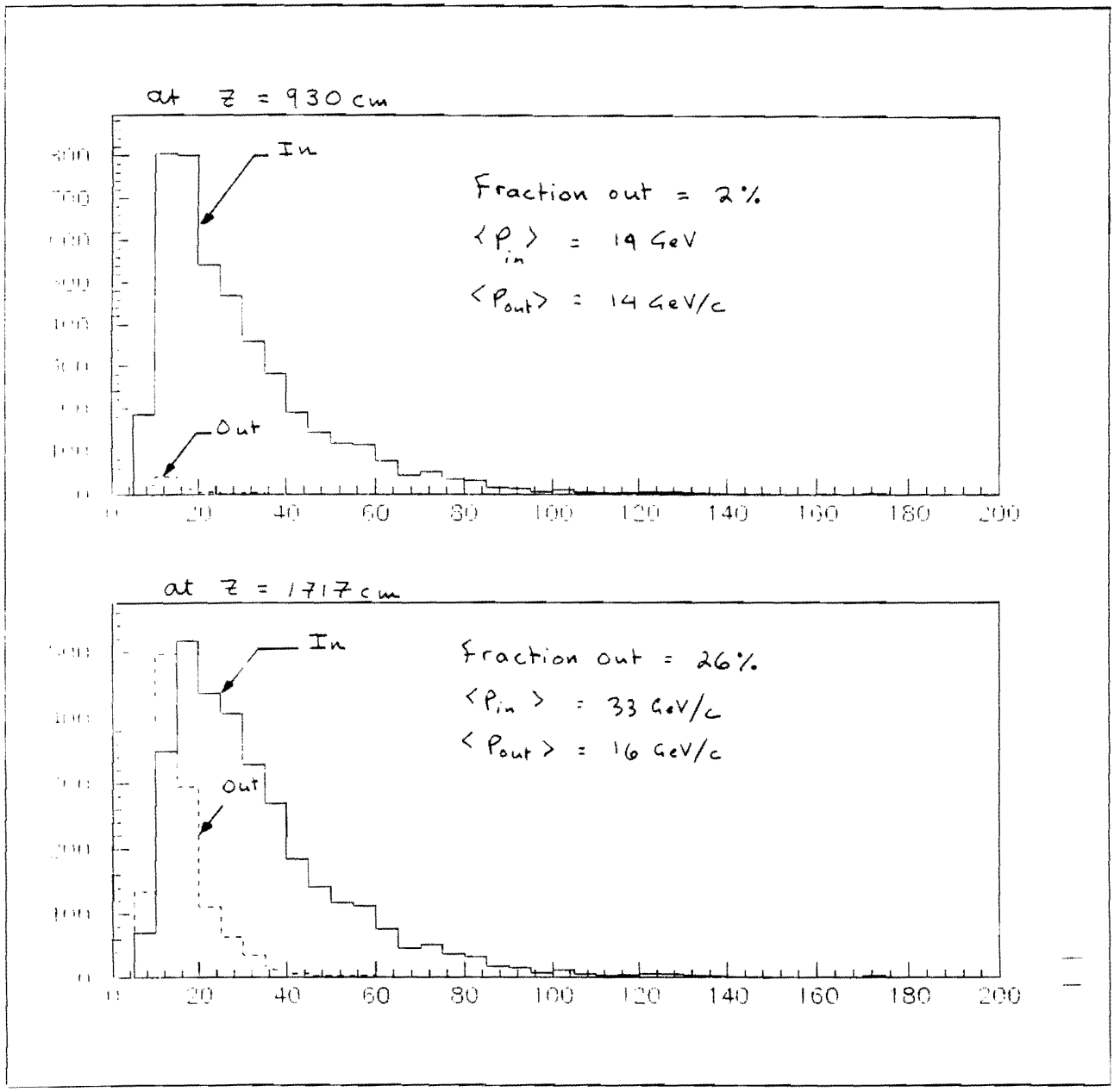
at z = 930 cm
In
Out
Fraction out = 2%
<P_in> = 19 GeV
<P_out> = 14 GeV/c
0
20
40
60
80
100
120
140
160
180
200
at z = 1717 cm
In
Out
Fraction out = 26%
<P_in> = 33 GeV/c
<P_out> = 16 GeV/c
0
20
40
60
80
100
120
140
160
180
200

3. Status of E791

E791 has reconstructed approximately 40% of its runs and many analyses are in progress. The plots shown below come from preliminary analyses, and many were shown publicly over the summer. Further analyses of these signals using larger data samples indicate that the estimates of the final sample sizes and the estimates of the precision for physics results are accurate.

In Figure 3-1 The $D^+ \rightarrow K^-\pi^+\pi^+$ (and c.c.) signal is shown as a function of kaon momentum. This sample was generated from the first 6% of the data to study Čerenkov identification efficiency, using somewhat tighter vertex separation and pointback cuts than will most analyses. The lightly shaded events are those with minimal pion identification and no kaon identification; the darkly shaded events are those with the same pion identification and a mild indication of kaon-like behavior by the kaon candidates in the Čerenkov detectors. Without considering kaon identification, the signal is 2832 ± 63 events over an integrated background ($\pm 40 MeV$) of 805 events. Requiring mild kaon identification, the signal is 1864 ± 47 events over an integrated background of 251 events. The sample without kaon identification has better statistics and a smaller fractional error, but the sample with kaon identification has a much better signal-to-background ratio. The choice of which sample to use depends on the analysis to be done. In general, kaon identification becomes important for decay modes which have fewer events and worse signal-to-background.

The benefit of Čerenkov identification of kaon candidates can be seen in Figure 3-2 where $D \rightarrow KK\pi$ candidates are shown with mild Čerenkov cuts on the two kaon candidates, Fig. 3-2(a), and with tighter Čerenkov cuts, Fig. 3-2(b). Although it is beneficial to cut more tightly for the generic $KK\pi$ signals, cutting on the invariant KK mass produces clean D^+ and $D_s \rightarrow \phi\pi$ signals using only the milder Čerenkov cut, Figures 3-2(d). Figure 3-3 illustrates the power of cutting on the kaon polar angle in the ϕ center-of-mass. This reduces the background by a factor of two while retaining 85% - 90% of the signal, giving a D_s signal of ap-

proximately 125 events over an integrated background of approximately 8 events (for 9% of the E791 data).

E791 also observes clean signals in semi-leptonic decay modes with either electrons or muons in the final state. Figure 3-4 show the "minimum mass" and $K\pi$ invariant mass distributions for 3-prong $K\pi l\nu$ candidates from the first 13% of the data. Clean $K^* l\nu$ signals are seen with electrons and with muons. The projected yields in these decay modes with these cuts are given in the tables shown as Figure 3-5. Further work with muon identification should allow cleaner signals with a small loss in statistics. Projections for the precision with which E791 will measure vector meson polarization in D^+ and D_s decays are shown in Figure 3-6. Projections for measuring the magnitudes of the *CKM* matrix elements V_{cs} and V_{cd} using other semi-leptonic decay modes are shown in Figures 3-7 and 3-8.

As an example of a rare decay search, E791 has looked for the FCNC decay $D^+ \rightarrow \pi^+\mu^+\mu^-$ (and c.c.) using well detached secondary 3-prong vertices containing a pair of muon candidates, and normalizing to the kinematically similar decay $D^+ \rightarrow K^-\pi^+\pi^+$. Figure 3-9 shows the $\pi\mu\mu$ invariant mass distribution for events in which the muon candidates have opposite signs (and for events in which the muon candidates have the same sign) from 10% of the data, and it shows the corresponding $D \rightarrow K\pi\pi$ invariant mass distribution as well. One event with opposite sign muons is observed in the D mass region. Given the measured pion misidentification rate, 0.6 background events are expected, leading to a 90% confidence level: $BR(D^+ \rightarrow \pi^+\mu^+\mu^-) < 3 \times 10^{-4}$. With the full data sample we can expect the upper limit to drop like $\sqrt{n}$, giving a limit near 10^{-4}.

A conservative estimate of the final E791 reconstructed charm sample size is summarized in the table shown as Figure 3-10. These numbers are all based on projections of signals already observed. As discussed for $D \rightarrow K\pi\pi$, the size of a particular signal depends in part on the specific analysis. Sometimes it will be most important to have an unbiased sample, and the signal-to-background ratio will not be critical. For other analyses, cleanliness will be more important. In

projecting to the proposed experiment, we are working from the numbers shown here, which correspond (roughly) to the cleanliness of the signals discussed.

Figure 3-1

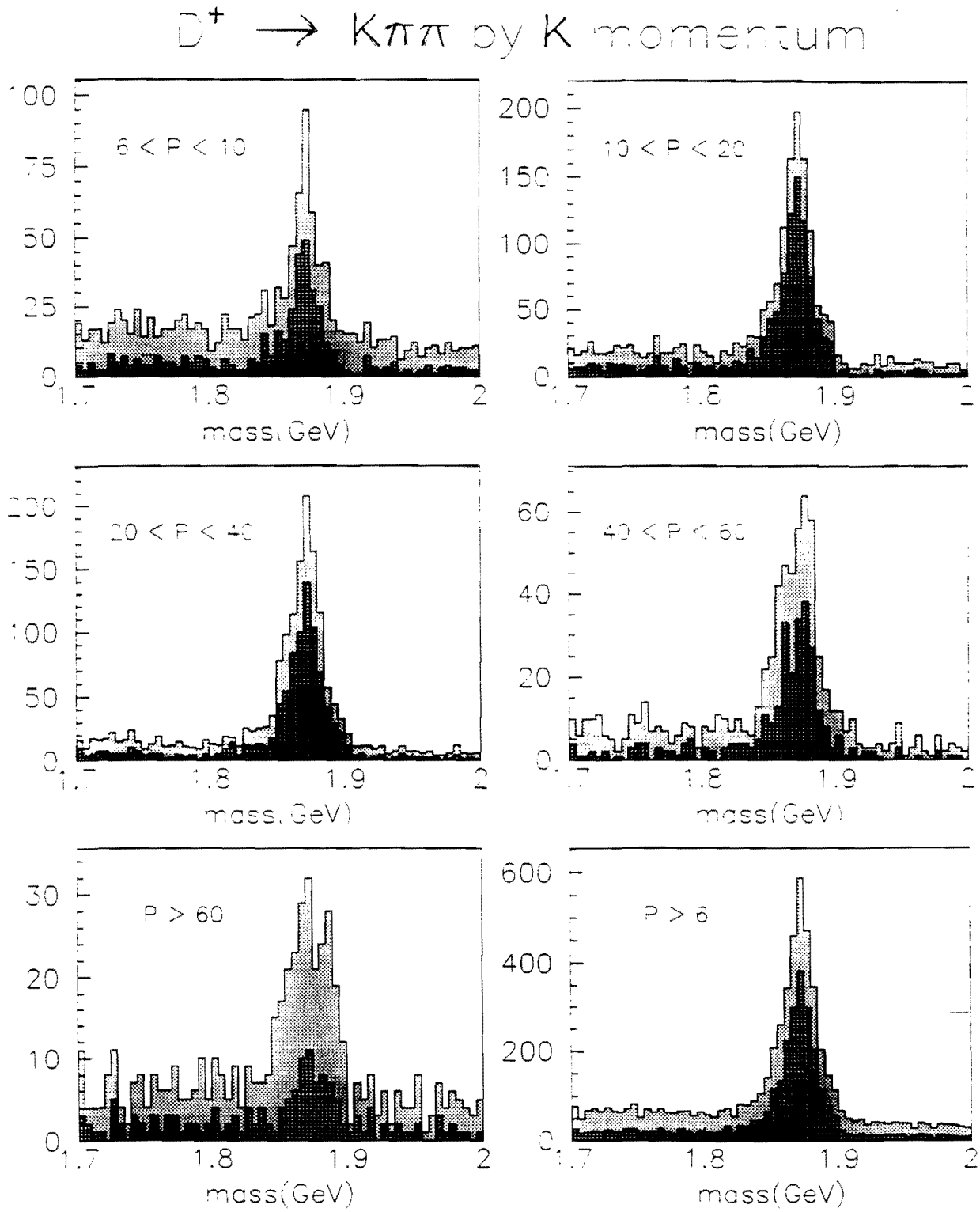
D+ → Kππ by K momentum
6 < P < 10
10 < P < 20
20 < P < 40
40 < P < 60
P > 60
P > 6
mass(GeV)
mass(GeV)
mass(GeV)
mass(GeV)
mass(GeV)
mass(GeV)

Figure 3-2

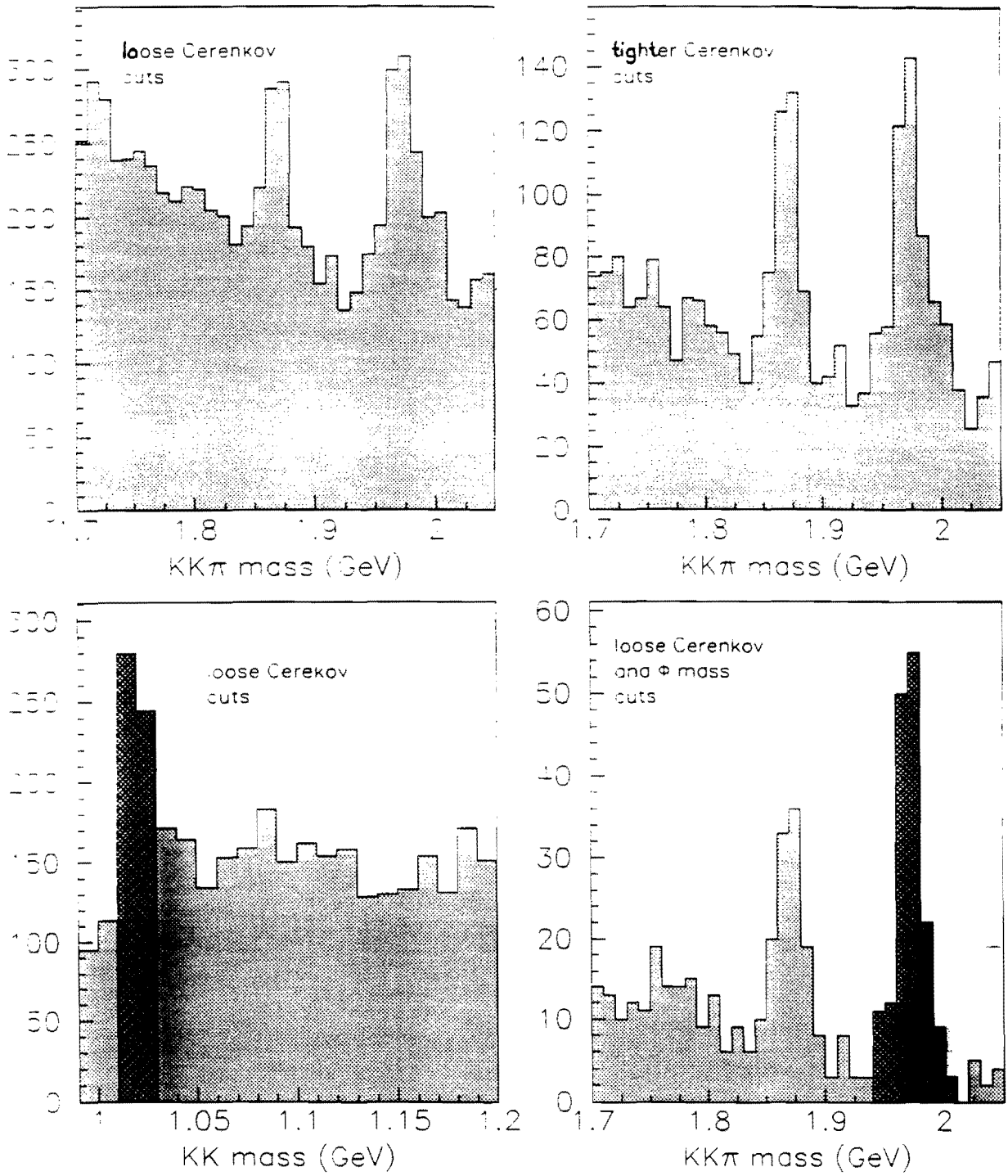
loose Cerenkov
cuts
KKπ mass (GeV)
tighter Cerenkov
cuts
KKπ mass (GeV)
loose Cerekov
cuts
KK mass (GeV)
loose Cerenkov
and Φ mass
cuts
KKπ mass (GeV)

Figure 3-3

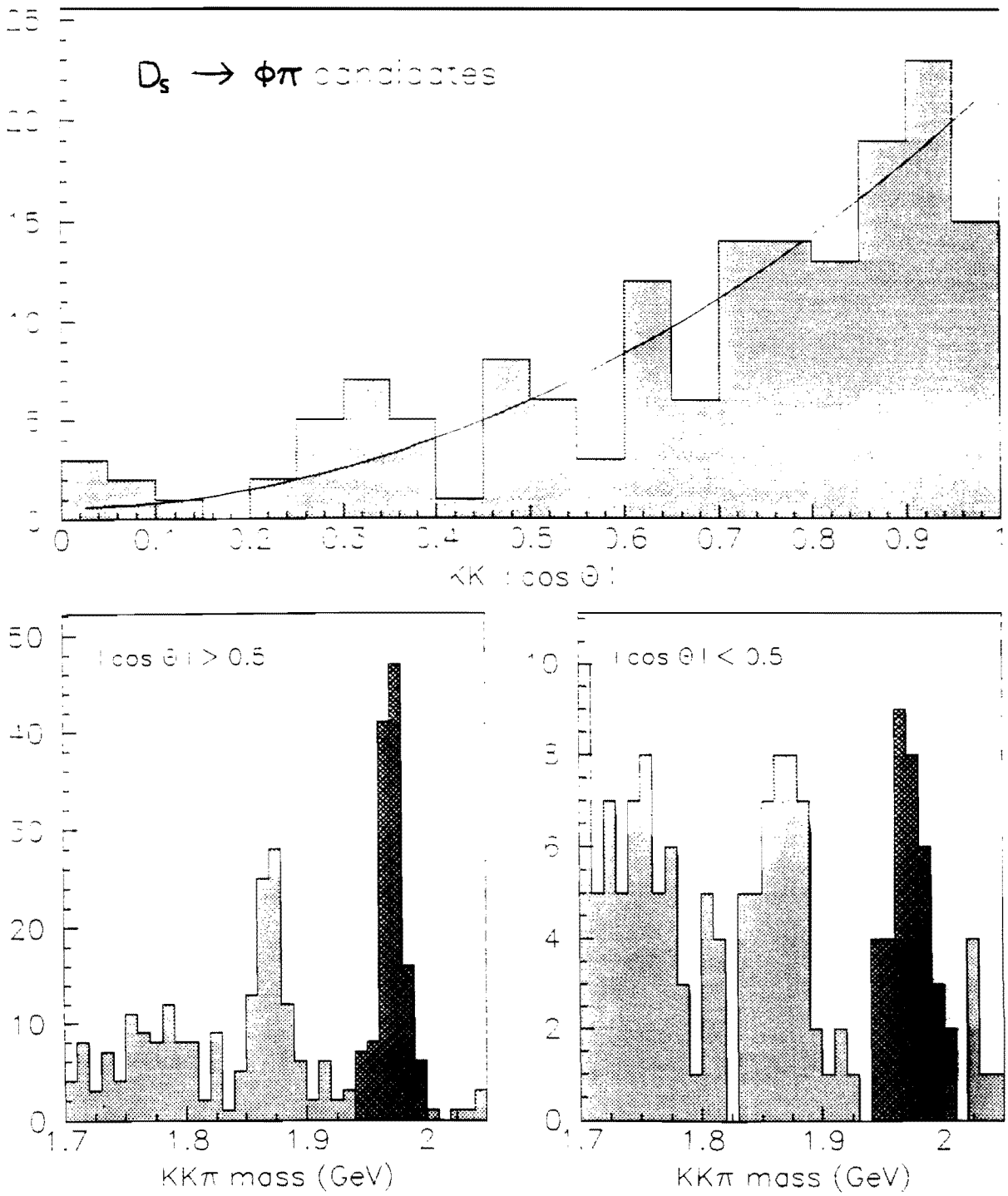
$D_s \rightarrow \phi\pi$ candidates
0.2
0.3
0.5
0.6
0.7
0.8
0.9
|cos Θ| > 0.5
|cos Θ| < 0.5
1.7
1.8
1.9
2
KKπ mass (GeV)
KKπ mass (GeV)

Figure 3-4

Minimum mass and invariant mass (Kπ)

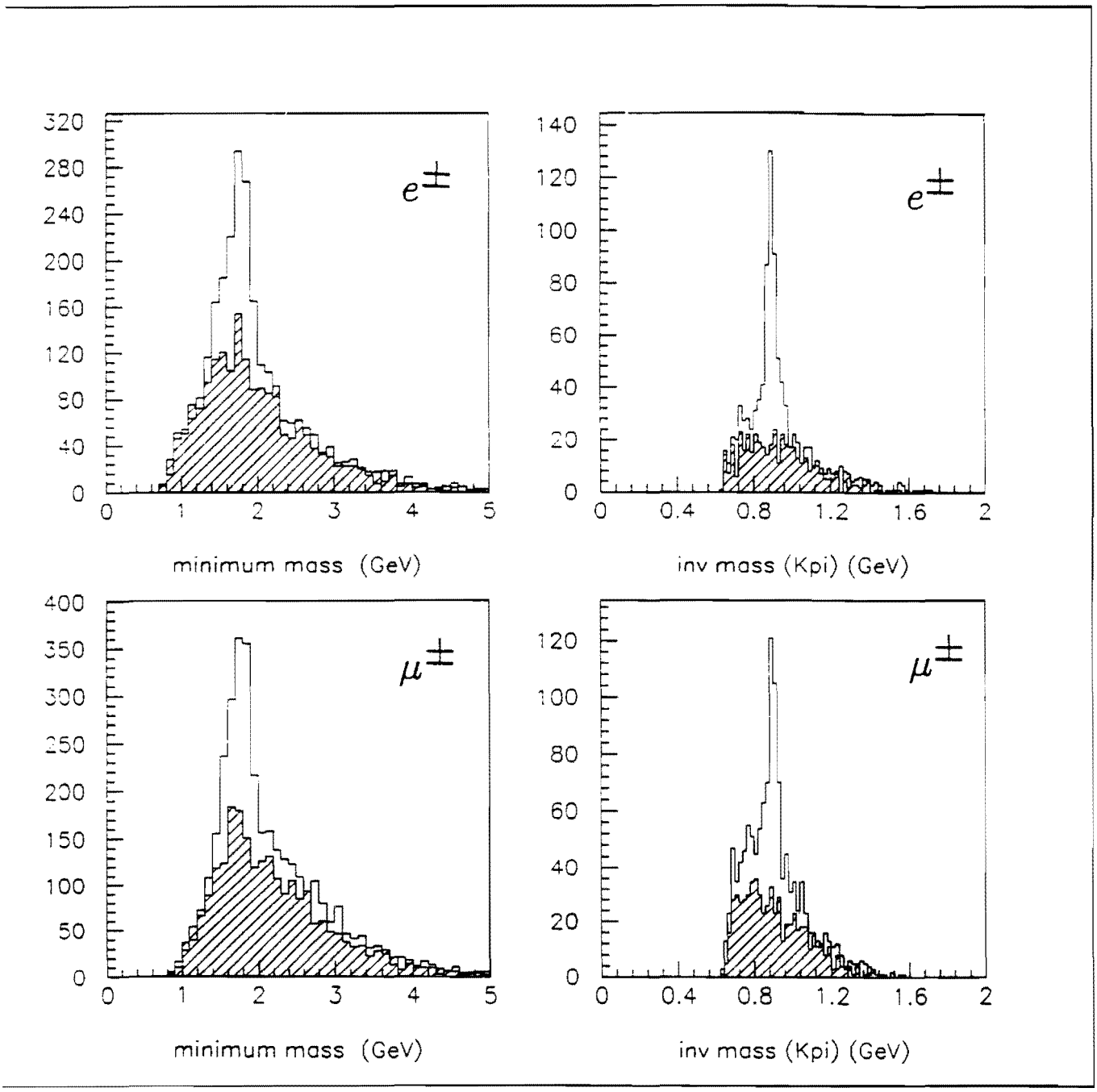

Figure 3-5

Preliminary signals (based on 13% of E791 data sample)

for $D^{\pm} \to \bar{K}^{*0} e^{\pm} \nu_e$

	loose cuts	tight cuts
# of right-sign events	421	365
# of wrong-sign events	93	60
# of signal events	328	305
significance (N_{sig}/σ_{sig})	14.5	14.8
signal/background ratio	4.5 ± 0.5	6.1 ± 0.8
expected yield in the entire data sample	≈ 2500	≈ 2300

for $D^{\pm} \to \bar{K}^{*0} \mu^{\pm} \nu_\mu$

# of right-sign events	448
# of wrong-sign events	142
# of signal events	306
significance (N_{sig}/σ_{sig})	12.6
signal/background ratio	3.2 ± 0.3
expected yield in the entire data sample	≈ 2300

Figure 3-6

Semi-Leptonic Decays to Vector Mesons

- $D \to Vl\nu$
  - has 3 form factors (V, A_1, A_2)

    or equivalently
  - has 3 helicity amplitudes (H_0, $H_\pm$)

- Look at the polarization:

$$\Gamma_L/\Gamma_T = \frac{\int P_V^* t |H_0(t)| dt}{\int P_V^* t \left[|H_+(t)|^2 + |H_-(t)|^2\right]} dt$$

MARK III	$0.5^{+1.0+0.1}_{-0.1-0.2}$
E691	$1.8^{+1.0}_{-0.4} \pm 0.3$
E653	$1.18 \pm 0.18 \pm 0.08$
E791	$\pm 0.05 \pm 0.05$

- also measure Γ_+/Γ_-

E653	$0.16 \pm 0.05 \pm 0.02$
E791	$\pm 0.015 \pm 0.010$

- also look at $D_S \to \phi l\nu$ with precision similar to E653 for $D^+ \to \overline{K}^{*0}\mu^+\nu_\mu$

Figure 3-7

Semi-Leptonic Decays and the *CKM* Mixing Matrix

PDG: with no unitarity constraint

$$
\begin{aligned}
|V_{ud}| &= 0.9744 \pm 0.0010 \\
|V_{us}| &= 0.2196 \pm 0.0023 \\
|V_{cd}| &= 0.204 \pm 0.017 \qquad (\pm 8\%) \\
|V_{cs}| &= 1.00 \pm 0.20 \qquad (\pm 20\%)
\end{aligned}
$$

$$\Gamma(D^0 \to K^- e^+ \nu_e) = |f_+(0)|^2 \, |V_{cs}|^2 \, (1.54 \times 10^{11}\,\mathrm{s}^{-1})$$

E791:	$\mathrm{BR}(D^0 \to K^- e^+ \nu_e)$	$\pm 3\%$ statistical
PDG:	$\mathrm{BR}(D^0 \to K^- \pi^+)$	$\pm 10\%$ absolute
PDG:	$\lvert f_+(0)\rvert^2$	$\pm 15\%$ absolute
PDG:	$\Gamma_{\mathrm{tot}}(D^0)$	$\pm 2\%$ absolute

$$\to \; |V_{cs}| \quad \pm 9\%$$

E791: $\mathrm{BR}(D^0 \to \pi^- e^+ \nu_e)$ $\pm 10\%$ statistical

$$\to \; |V_{cd}| \quad \pm 10\%$$

Figure 3-8

$|V_{cs}|$, Another Approach

$$\text{E791}: \quad \frac{\text{BR}(D^0 \to \pi^- e^+ \nu_e)}{\text{BR}(D^0 \to K^- e^+ \nu_e)} \quad \pm 10\%$$

$$\frac{|V_{cd}|^2}{|V_{cs}|^2} = 0.51 \frac{|f_+^K(0)|^2}{|f_+^\pi(0)|^2} \frac{\text{BR}(D^0 \to \pi^- e^+ \nu_e)}{\text{BR}(D^0 \to K^- e^+ \nu_e)}$$

combine with existing $|V_{cd}|$,

$$\to \quad |V_{cs}| \quad \pm 6\% \quad \pm 8\%$$

Figure 3-9

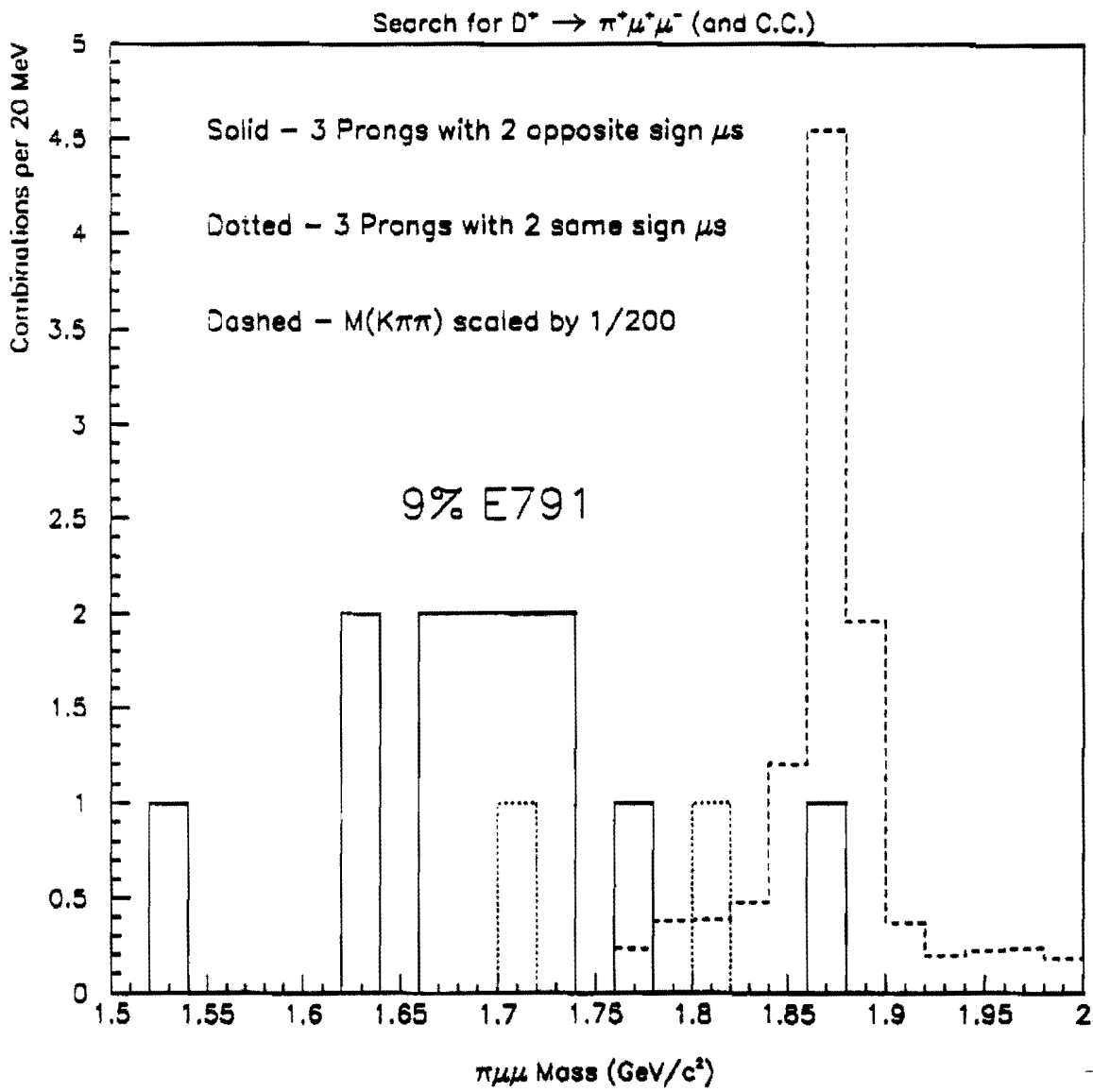
Search for $D^+ \rightarrow \pi^+\mu^+\mu^-$ (and C.C.)
Combinations per 20 MeV
Solid – 3 Prongs with 2 opposite sign μs
Dotted – 3 Prongs with 2 same sign μs
Dashed – M(K$\pi\pi$) scaled by 1/200
9% E791
$\pi\mu\mu$ Mass (GeV/c^2)
0
0.5
1
1.5
2
2.5
3
3.5
4
4.5
5
1.5
1.55
1.6
1.65
1.7
1.75
1.8
1.85
1.9
1.95
2

Figure 3-10

Projected Final Sample Size (Loose Cuts)

Final States with All Charged Tracks

$D^0 \rightarrow K^-\pi^+$	70k
$D^0 \rightarrow K^-\pi^-\pi^+\pi^+$	35k
$D^+ \rightarrow K^-\pi^+\pi^+$	60k
other D^0, D^+, D_S, and Λ_C	$>$ 10k
final states with neutral V^0's	$>$ 10k
D^0, D_S, $D^+ \rightarrow K^0_S X$	
Λ_C, $\Xi_C \rightarrow \Lambda X$. $K^0_S X$	
semi-leptonic final states	$>$ 10k
with $\mu^\pm$	
with $e^\pm$	
total	**$\approx$ 200k**

4. P829 Goals

The major strength of the experiment we are proposing will be its ability to generate vary large signals of charmed mesons which decay hadronically to states containing only charged particles, or which decay semi-leptonically to states containing charged particles and neutrinos. Here we present some of the physics topics for which we expect our results to have substantial impact.

4.1. Semi-leptonic Decays

The proposed experiment will be able to systematically study semi-leptonic decays of D mesons at a level which will allow direct comparisons of decay rates and form factors at the 5% to 10% level. The largest signals will come from $D^+ \to \overline{K}^{*0} l\nu$ and $D^0 \to K^- l\nu$, but $D_S \to \phi l\nu$, $D^0 \to K^{*-} l\nu$, and $D^+ \to \overline{K}^0 l\nu$ signals will also be large enough to make high precision measurements.

E791 expects to measure the polarization of the K^* in $D^+ \to \overline{K}^{*0} l\nu$ decays with 5% statistical errors using both electrons and muons. The proposed experiment should be able to push the statistical precision to the 1% level. Additionally, using a cleaner and more efficient muon detector should allow us to reduce E791's anticipated 5% systematic error in the muon sample to a few percent. Similarly, we should be able to measure the polarization in $D_S \to \phi l\nu$ with 5% precision, and the polarization in $D^0 \to K^{*-} l\nu$ followed by $K^{*-} \to K_S^0 \pi^-$ with a few percent precision. By measuring the decay rates and form factors for the corresponding semi-leptonic decays of the three D's, we will provide theorists with strong constraints for their models.

Where E791 anticipates measuring the ratio of branching ratios $\mathrm{BR}(D^0 \to K^- e^+ \nu)/\mathrm{BR}(D^0 \to K^- \pi^+)$ with 2% statistical precision, the proposed experiment will make the same measurement with fraction of a percent statistical error. More interestingly, we should be able to measure the mass of the pole in the vector form factor with a few percent error, about 25 MeV, assuming a single-pole form. E791 anticipates measuring the ratio $\mathrm{BR}(D^0 \to \pi^- l\nu)/\mathrm{BR}(D^0 \to K^- l\nu)$ with

10% precision. With 15 - 25 times as much data as E791, we should be able to measure this ratio with 2% - 4% precision, including systematic errors. This leads to a statistical error on the ratio of relevant *CKM* matrix elements, $|V_{cd}|/|V_{cs}|$, of 1% - 2%. The uncertainty in this ratio will be dominated then by the theoretical uncertainty in the ratio of form factors at $q^2 = 0$, $|f_+^K(0)|/|f_+^\pi(0)|$ (see Figure 3-8).

4.2. Doubly Cabibbo-Suppressed Decays and D^0-$\overline{D}^0$ Mixing

Several experiments have reported statistically significant signals for doubly Cabibbo-suppressed decays of the D^0 and D^+. E791 should be able to observe such decays ($D^0 \to K^+\pi^-$, $D^+ \to K^+\pi^+\pi^-$, $D^+ \to K^+K^+K^-$, etc.) at the 3 - 5 σ level given the background rates observed so far. The proposed experiment should have sufficient statistics to measure the "inclusive" DCSD rates very well, and to study the resonant substructure of final states such as $K^+\pi^+\pi^-$. Additionally, because the experiment will measure decay times with good precision, it will be possible to separate DCSD and D^0-$\overline{D}^0$ mixing rates.

The best published limit on D^0-$\overline{D}^0$ mixing, ($r_{\rm mix} < 0.37\%$), which comes from E691, is still several orders of magnitude (in $r_{\rm mix}$) from the short-distance scale Standard Model prediction [1] ($r_{\rm mix} \sim 10^{-7}$). While some authors have argued that intermediate hadronic states can increase the rate of mixing by orders of magnitude [2 – 3], recent theoretical work questions that conclusion [4 – 5]. This implies a big discovery window for new physics. The recent CLEO II observation [6] of wrong-sign decays calls for fixed-target experiments which measure decay times to determine whether the signal is due to DCSD decays or due to mixing. Assuming that it is due to DCSD decays, one gets an irreducible background to mixing. If the CLEO signal is due to DCSD's, then E791 should be able to set a limit on $r_{\rm mix}$ at the 0.10 – 0.15% level, while E687 should get to the 0.2 – 0.3% level. With its higher statistics, the proposed experiment should be able to reduce this limit to $r_{\rm mix} < 2 - 4 \times 10^{-4}$.

References for 4.2

[1] See, for instance, E. D. Commins and P. H. Bucksbaum "Weak Interactions of leptons and quarks", Cambridge University Press, New York, 1983.

[2] L. Wolfenstein, Phys. Lett. **B164**, 170 (1985).

[3] J. F. Donoghue et al., Phys. Rev. **D33**, 179 (1986).

[4] H. Georgi, Phys. Lett. **B297**, 353 (1992).

[5] T. Ohl, G. Ricciardi and E. H. Simmons, Nucl. Phys. **B403**, 605 (1993).

[6] T. Browder, Cornell University, private communication.

4.3. *CP* Violation and Flavor-Changing-neutral-Currents

The Standard Model predicts that direct *CP* violation (observed as the fractional difference between decay rates of particle and anti-particle to charge conjugate final states) will be of order 0.1% or less in the single Cabibbo-suppressed D decays. (In the Standard Model, *CP* should be an exact symmetry for Cabibbo-allowed and DCSD D decays.) Physics beyond the standard model might contribute *CP* violating amplitudes to decay rates, and there is a large window for observing new physics. The proposed experiment should produce an 8,000 - 12,000 $D^0 \to K^+K^-$ event signal and a similar $\overline{D}^0 \to K^+K^-$ signal from the decay chain $D^{*\pm} \to D\pi$ with integrated backgrounds less than half as large as the signals. Assuming 1 – 2 σ statistical fluctuations, the proposed experiment will set an upper limit on *CP* violation of 2 – 4% in this decay mode. Extrapolating from the $D^\pm \to \phi\pi$ peak seen in Figure 3-3, the proposed experiment should produce 8,000 - 12,000 event signals in each of $D^+ \to \phi\pi^+$ and $D^- \to \phi\pi^-$, with less than 20% backgrounds, leading to an upper limit on *CP* violation a bit more stringent than that for $D \to KK$. Other decays, such as $D \to \pi\pi$ and $D \to K^*K$, will have comparable size signals, but somewhat higher backgrounds, so the limits on direct *CP* violation for those decays will be less stringent. However, the *CP* violating amplitudes which contribute to an asymmetry in one decay mode need not contribute comparably

to an asymmetry in another decay mode, so it will be important to search for CP violation in all decay modes where we have sensitivity better than 10%.

4.4. Topics in B Physics

We have also evaluated the reach of our proposed experiment for studying some topics in B physics. Using the integrated luminosity assumptions discussed earlier, and a $b\bar{b}$ cross-section of 15 nb for a 500 GeV π^- beam, approximately 500,000 $b\bar{b}$ pairs will be produced in our target while the detector is live. Monte Carlo studies which allow for geometric acceptance, triggering efficiency, tracking efficiencies, vertexing efficiencies, and particle identification indicate that we can reconstruct a sample of approximately 50 $B_s \rightarrow D_s^{(*)}\mu\nu$ events with the D_s decaying into $KK\pi$ and 30 events with an electron instead of a muon. In addition, we expect to reconstruct about 20 events of the type $B_s \rightarrow D_s^{(*)}$ + 1 or 3 charged pions. These Monte Carlo studies indicate that we can reconstruct a similar number of $\Lambda_b \rightarrow \Lambda_c l\nu$, $\Lambda_b \rightarrow \Lambda_c\pi$, and $\Lambda_b \rightarrow \Lambda_c\pi\pi\pi$ events. Neither CLEO II nor either of the existing hadron collider experiments is sensitive to these decays, so we have the potential to make a unique contribution in B decay physics.

Additionally, we expect that we can fully reconstruct between one and two hundred B_d and B_u decays, and partially reconstruct more B decays where we observe a fully reconstructed D which does not point to the primary vertex but which does point to a secondary vertex outside the target region. Beauty events can also be identified in which two high p_T leptons are reconstructed which both miss the primary vertex and do not intersect each other. Using these signals, we should be able to study the total cross-section for producing B's with a 500 GeV π^- beam, the differential B cross-sections as functions of Feynman x and transverse momentum, and the relative production rates for B_d, B_u, B_s, and Λ_b.

5. Reaching the Goals

One measure of the "reach" of our proposed experiment is the number of charmed meson decays that will be reconstructed in decay modes that are currently reconstructed well by E791, such as $D \rightarrow K2\pi$. For these modes, we expect the new experiment to reconstruct approximately 20 times as many decays as E791. Upgrades of the wire chamber tracking, the particle id systems, and the vertex detector will allow even larger increases in statistical power over E791 in other final states; for example, high multiplicity final states and final states including leptons, especially muons.

In this section we review how our proposed experiment will reach 20 times E791 for decays such as $D \rightarrow K2\pi$.

5.1. Record More Events ($\times 3$)

E791 wrote 20 billion events to tape during the 1990 fixed target run. The experiment collected just under 10,000 events per beam second and ran for just over 2×10^6 seconds. We will collect data at 20,000 events per beam second and write it to 8mm tape at twice the density as did E791. We estimate we will spend one-half of the scheduled 10 month run debugging the detector, and one-half of the run logging data. This implies a 152 day run, or 21.7 weeks. If we assume 100 hours of usable beam per week, this translates into 3.15×10^6 beam seconds ($21.7 \times 100 \times 3600 \times 23/57$). For this estimate, we assume that we will log data for 3×10^6 beam seconds. Therefore, we expect to log a total of 60 billion events to tape, a factor of three more than E791. It should be noted that since we will use higher density 8mm tape, this data set will require only 50% more tape than was used by E791.

5.2. Increase the E_T Trigger Threshold ($\times 2.4$)

E791 used an E_T trigger with a 4 GeV threshold. This served to reject "interaction" triggers caused by Landau fluctuations in the signal from the interaction counter caused by uninteracted beam particles, but it accepted the great majority of interactions in the targets. We have studied the effect of higher E_T thresholds using E791 data. Each event record contains digitized information which allows one to calculate its E_T as measured for the E_T trigger. We have histogrammed E_T for a sample of data from E791. As expected, this histogram shows an abrupt turn-on at 4 GeV. We have also histogrammed E_T for events containing reconstructed charmed particles in a variety of different decay modes. We can calculate the charm enhancement a given E_T cut would provide by dividing the fraction of charm events with E_T greater than the cut by the fraction of all events with E_T greater than the cut. At the same time, we can calculate the increase in luminosity that would be required for a given E_T trigger in order to maintain a constant trigger rate. Typical results are shown in figure 5-1. We estimate that an E_T cut of 8.4 GeV is 72% efficient for charm events and 30% efficient for all events with E_T above 4 GeV. This corresponds to an enrichment of the fraction of events on tape containing charm of a factor of 2.4 with respect to E791. We believe this to be an extremely reliable estimate, since it is calculated directly from E791 data using E_T as measured by the TPL calorimetry.

5.3. Increase the Charm Reconstruction Efficiency ($\times 1.7$)

As noted in section 2.2, we have begun to study the charm reconstruction efficiency of our proposed spectrometer using E791 data and the E791 Monte Carlo. We generated 75000 $D \rightarrow K2\pi$ decays using Pythia, and simulated the response of the existing E791 spectrometer. A total of 4313 decays were reconstructed (Figure 5-2). We then simulated the response of an improved detector, which differed from the E791 detector in that the drift chambers were efficient, did not have a large dead central hole caused by radiation damage, and had 180μ resolution. We also

modified the description of the SMD planes for which we are planing electronics upgrades so that their performance matched the performance of the E791 beam SMD planes. The result is shown in Figure 5-3. A total of 7623 decays were reconstructed. The improvement in reconstruction efficiency was 7623/4313 = 1.77.

5.4. Use Higher-A Target Material ($\times 1.5$)

Since the charm production cross-section goes approximately like A^1 (G. Alves et al., PRL 70, p722, 1993), while the total inelastic cross- section is approximately proportional to $A^{.75}$ (D. Barton et al., PRD 27, P2580, 1983), the fraction of events containing charm can be expected to be proportional to $A^{.25}$. High A materials are also denser than low A materials, which means that a high A target is thinner than a low A target of the same number of interaction lengths. This is potentially a large advantage for the reconstruction of particles, such as Λ_c, with very short lifetimes. These advantages must be traded off against the fact that high A materials are also high Z, which means that they cause much more multiple scattering and photon conversions than equivalent low A targets. We are still in the process of understanding the trade-offs associated with different target materials. Currently, our best guess is that we will select copper as a target material. This will yield a charm enrichment with respect to the carbon targets used in E791 of a factor of 1.5 ($63^{.25}/12^{.25}$).

5.5. Optimize the Target Geometry ($\times 1.2$)

We will use only a single foil target to optimize the fiducial volume for charmed meson decays. E791 finds that secondary vertices are efficiently separated from primary vertices when the separation is at least 4 - 6 mm, but not below. The vertex resolution from pointing tracks into the foils is also much better than the foil thickness divided by $\sqrt{12}$, so there is no substantial advantage in using a series of thinner foils spaced over 8 centimeters, as E791 did. There are at least three

advantages to using a single foil – that all the charm decays beyond the end of the foil occur in air, that the multiple scattering between the charm decay vertices and the SMD system is reduced, and that the position of the target relative to the vertex detector system may be better optimized. Secondary interactions in the foils downstream of the foil containing a primary interaction often mimic charm decays. Most of the analyses done with the E791 data have excluded such vertices as charm candidates, and this reduces the signals as much as 30% (for the relatively long-lived D^+). Because there will be no foils between the charm decay vertex and the first plane of the SMD system, there will be less multiple scattering than in E791. This will improve vertex resolution, and therefore reduce backgrounds. Since we have not yet decided on a target material or thickness, we have not been able to reliably quantify the increase in charm yield which we will gain by optimizing the target configuration. We believe that 20% relative to E791 is a safe estimate.

The product of these five terms is: $3 \times 2.4 \times 1.7 \times 1.5 \times 1.2 = 22$

5.6. Beam and Target

In order to maximize the heavy quark production cross sections, and maximize the yield of short lived states, we would like to operate with the highest energy pion beam available. In PEast, this is 500 GeV/c π^-. In order to maintain a trigger rate of 20 KHz, we will require approximately 130 KHz of interactions in our target. We calculate this number as follows: 1) E791 triggered on approximately 75% of the total cross section; 2) Our E_T trigger will reject a factor of 3.3 more events than the 4 GeV trigger used by E791; 3) The detector livetime will be 70%. Thus, $(20 \text{ KHz} \times 3.3)/(.75 \times .7) = 126$ KHz.

E791 ran with 2×10^{12} protons/pulse incident on the PEast pion production target. This yielded a 2 MHz 500 GeV π^- beam at TPL, 1.5 MHz of which was inside a $1cm^2$ "good" beam spot. We believe that radiation safety limits will allow

us to increase this to between 3 and 4 $\times 10^{12}$. An intensity of 3.5 $\times 10^{12}$ per spill on the production target will yield a "good" beam of 2.6 MHz. A 5% interaction length target will result in the desired 130KHz of interactions. If studies of Monte Carlo and E791 data indicate that a higher E_T threshold is desirable, or that a thinner target is desirable, we will adjust the target thickness and/or increase the beam flux by lowering the beam energy slightly.

Figure 5-1

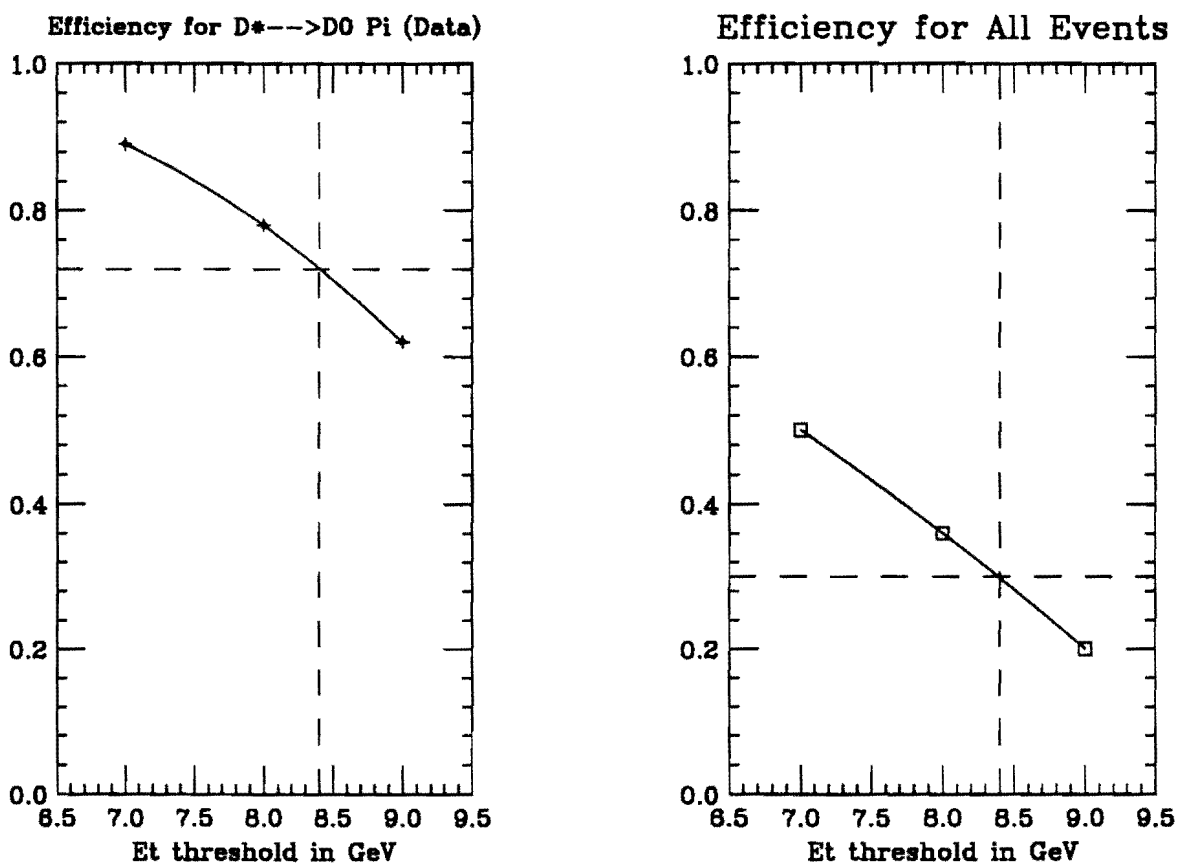
Efficiency for D*-->D0 Pi (Data)
1.0
0.8
0.6
0.4
0.2
0.0
6.5 7.0 7.5 8.0 8.5 9.0 9.5
Et threshold in GeV
Efficiency for All Events
1.0
0.8
0.6
0.4
0.2
0.0
6.5 7.0 7.5 8.0 8.5 9.0 9.5
Et threshold in GeV

Figure 5-2

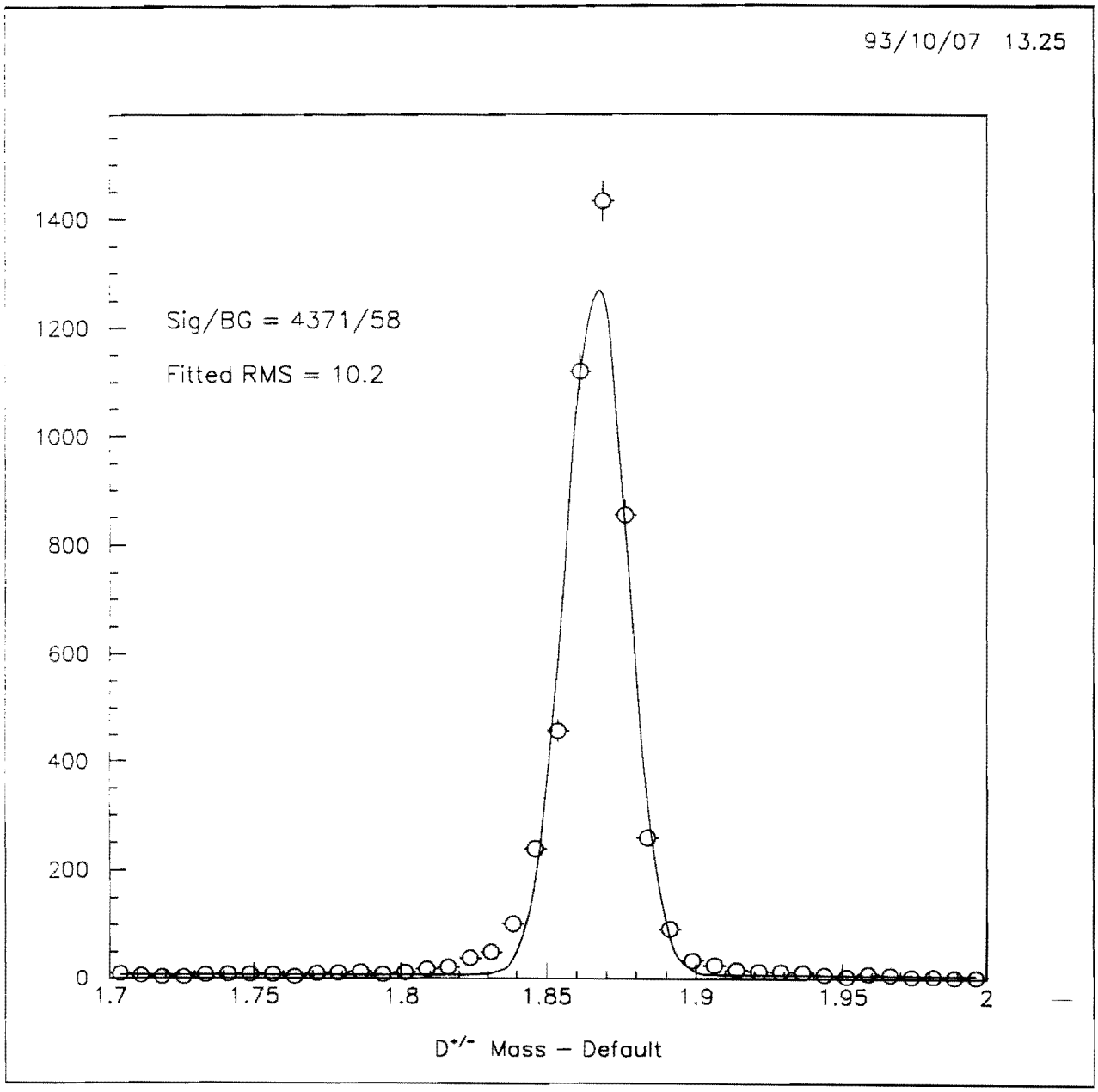
93/10/07 13.25
Sig/BG = 4371/58
Fitted RMS = 10.2
1400
1200
1000
800
600
400
200
0
1.7
1.75
1.8
1.85
1.9
1.95
2
D+/- Mass – Default

Figure 5-3

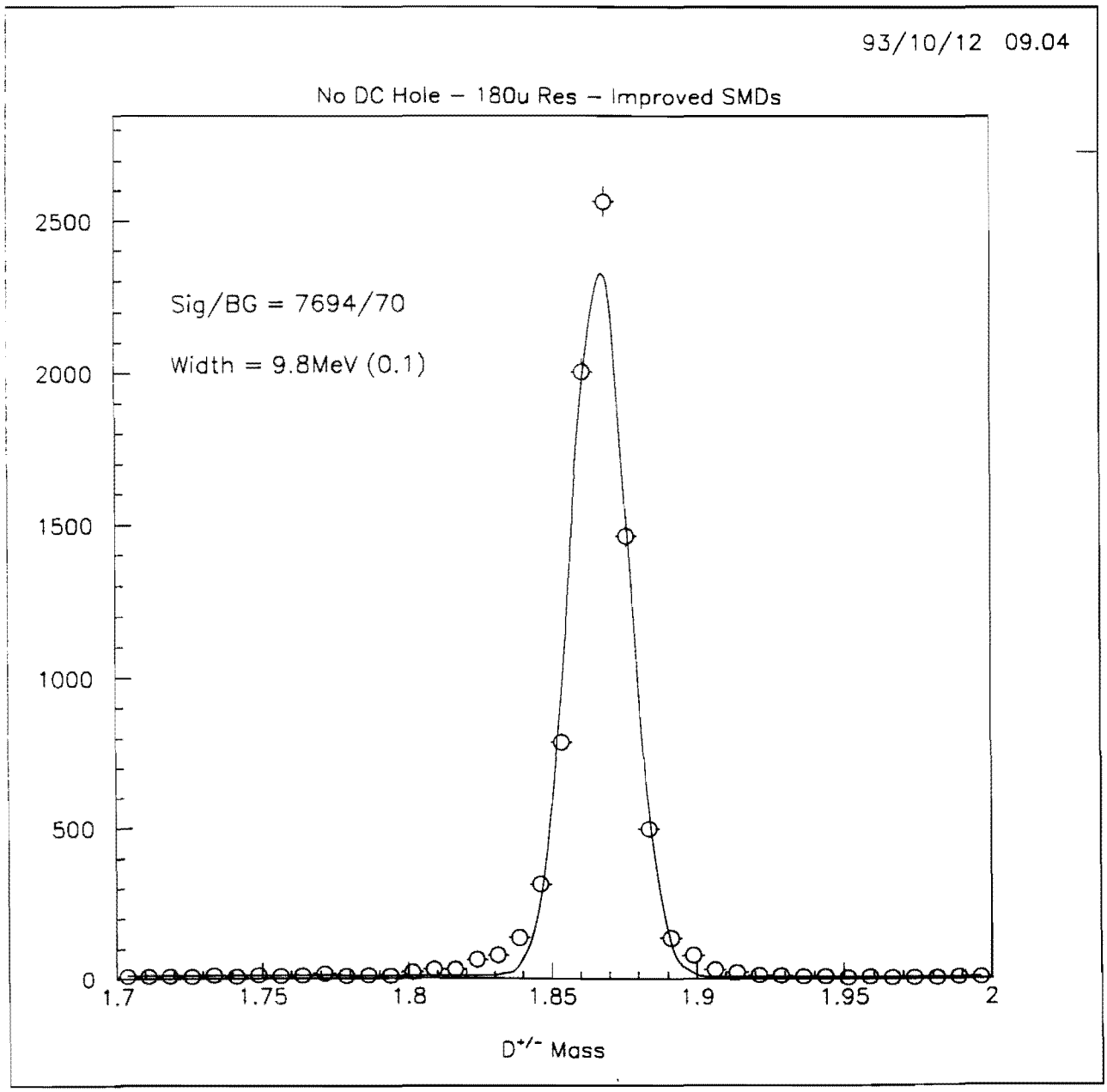
93/10/12 09.04
No DC Hole – 180u Res – Improved SMDs
Sig/BG = 7694/70
Width = 9.8MeV (0.1)
2500
2000
1500
1000
500
0
1.7
1.75
1.8
1.85
1.9
1.95
2
D+/- Mass

6. Comparison With Other Experiments

Comparing experiments with diverse goals is always difficult. Simply comparing the total yields of reconstructed charm does not allow for the cleanliness of signals or for the number of channels being studied. Because the primary goal of P829 is the study of charmed meson decays to all charged particles (and missing neutrinos), we illustrate the power of our experiment relative to others which have studied similar physics, and which are planning to study similar physics, by looking at the statistical significance of the $D^+ \rightarrow K^-\pi^+\pi^+$ signal. While P829 will not compete with E831 or CLEO II in measuring charm with π^0's or η's in the final state, it does promise the greatest sensitivity for a wide variety of physics measurements.

Experiment	Total Reported/Projected Charm Signal	Significance of $D^+ \rightarrow K^-\pi^+\pi^+$ Signal
E691	10,000	40 σ
E687	100,000	70σ
E791	200,000	160σ
E831	1,000,000	220σ
CLEO II	1,000,000	445σ
P829	4,000,000	**715σ**

Table 6-1: Comparison of charm yields from various experiments. The numbers for E691 and E687 are based on published results. The numbers for E791 come from extrapolating signals from the reconstructed data. The numbers for E831 come from assuming it reconstructs ten times the signal of E687 with the same cleanliness, as projected in that proposal. The numbers for CLEO II come from extrapolating their $D \rightarrow K\pi$ signal from that observed at 680 pb^{-1} to 20 fb^{-1}, the largest integrated luminosity they might accumulate over the next five years, and assuming their $D^+ \rightarrow K^-\pi^+\pi^+$ signal will be comparably clean. The numbers for

P829 come from assuming it will reconstruct 20 times as much signal as E791.

7. Resources Required

7.1. New Equipment

In addition to the costs associated with merging apparatus from E690 into TPL, we anticipate the following major costs:

	Quantity	Unit Cost	Total
Exabyte 8500 8mm Tape Drives	48	$3K	$144K
VME Processors w/SCSI Interfaces	12	$5K	$60K
Event Buffer Interfaces	24	$.5K	$12K
80MB VDAS FIFO Buffer Systems	4	$15.2K	$61K
Damn Yankee Controllers	20	$.5K	$10K
SMD Scanners	92	$.4K	$37K
5cm 25/50u SMD Wafers Bonded to Fanout	2	$10K	$20K
QPA02-based SMD Preamplifiers	8000 ch	$4/channel	$32K
SMD Disc/Latch Modules	10K ch	$16/channel	$160K
		Total	$536K

7.2. Analysis

The current E791 event reconstruction takes 12 MIPS-seconds per event. Although we believe that spectrometer improvements will reduce this time, we use it to estimate the computing resources necessary to analyse the 60 billion events we expect to collect:

$$(60 \times 10^9 \times 12 \text{ MIPS-sec})/(3 \times 10^7 \text{ sec/year}) = 24{,}000 \text{ MIPS-years.}$$

We request dedicated use at Fermilab of 12,000 MIPS of computing for the period of time required to reconstruct our data. At $50/MIPS, this represents a $600K request. Assuming that our University collaborators are able to match this facility with an additional 12,000 MIPS's (which is a smaller fraction of the total required that has been provided by E791 collaborating institutions), it will be possible to reconstruct all of our data in approximately one year.

8. Summary

The experiment we propose builds on past experiences with the Tagged Photon Spectrometer, the E690 spectrometer, and the E789 spectrometer. Starting with E791's signals, we have extrapolated to the expected yield. We will accumulate the world's largest sample of reconstructed charm. We will use this to study the detailed properties of charmed meson decays and other topics in heavy quark physics. We will make precise measurements which will constrain phenomenology within the Standard Model (charm decay dynamics, spectroscopy, and production). We will search for phenomena beyond the Standard Model in channels where we have greater sensitivity than other experiments (non-standard CP violation, $D^0/\overline{D^0}$ mixing, and flavor changing neutral currents).

Most of the hardware needed to prepare TPL for a higher rate experiment exists at Fermilab and has been used successfully in other experiments. This reduces the cost of preparing the next generation experiment, and provides some assurance that the detector can be made to operate as advertised in a timely way. In addition, the collaboration which has formed so far has the experience and strength necessary to commission, operate, and analyse the experiment successfully. The experiment we propose will help maintain Fermilab's leadership in charm physics, and will lay the groundwork for future ultra-high rate heavy quark experiments.